

AperTO - Archivio Istituzionale Open Access dell'Università di Torino

Effect of structure and microstructure on the thermoelectric properties of Yb_{0.19}Co₄Sb₁₂ alloy

This is the author's manuscript

Original Citation:

Availability:

This version is available <http://hdl.handle.net/2318/149069> since

Publisher:

Springer International Publishing

Terms of use:

Open Access

Anyone can freely access the full text of works made available as "Open Access". Works made available under a Creative Commons license can be used according to the terms and conditions of said license. Use of all other works requires consent of the right holder (author or publisher) if not exempted from copyright protection by the applicable law.

(Article begins on next page)



UNIVERSITÀ DEGLI STUDI DI TORINO

This is an author version of the contribution published on:

Questa è la versione dell'autore dell'opera:

*A. Castellero et al., Proceedings of the 11th European Conference on Thermoelectrics:
A. Amaldi and F. Tang (editors), Springer International Publishing, 2014, pagg. 1-9*

The definitive version is available at:

La versione definitiva è disponibile alla URL:

http://link.springer.com/chapter/10.1007/978-3-319-07332-3_1

Effect of structure and microstructure on the thermoelectric properties of $\text{Yb}_{0.19}\text{Co}_4\text{Sb}_{12}$ alloy

A. Castellero^{1,*}, M. Ostorero¹, A. Ziggotti², M. Brignone², M. Baricco¹

¹ Dipartimento di Chimica and NIS, Università degli Studi di Torino, Torino, Italy

² Centro Ricerche FIAT, Orbassano (TO), Italy

* Corresponding author: Alberto Castellero, tel.: +390116707097, fax: +390116707855, e-mail:

alberto.castellero@unito.it

Abstract

In this work, we report results about the synthesis and characterization of the n-type $\text{Yb}_{0.19}\text{Co}_4\text{Sb}_{12}$ thermoelectric alloy that is among the most promising materials for automotive applications with a value of ZT ranging around 1 at 600 K.

Samples preparation consisted of a sequence of three steps: 1) a solid/liquid reaction between the individual elements at 660°C in a resistance furnace; 2) complete melting in an induction furnace; 3) annealing at 730°C in a resistance furnace for 0.75h, 1.5h, 3h and 6h.

The non-annealed samples consist of a mixture of Sb, YbSb_2 , CoSb, CoSb_2 and CoSb_3 . Only a fraction (about 50%) of the thermodynamically stable CoSb_3 -type phase could be obtained by free cooling of the melt. This is due to the complex solidification path, involving two peritectic transformations, that does not allow the system to reach the equilibrium.

Annealing at 730°C promotes the formation of the desired CoSb_3 -type phase up to fractions around 98% after 3-6 hours.

Thermoelectric properties were measured between 300 K and 500 K. Annealing brought to a progressive increase of the absolute values of the Seebeck coefficient, as a consequence of the higher fraction of the $\text{Yb}_x\text{Co}_4\text{Sb}_{12}$ thermoelectric phase. In the case of electrical conductivity, no clear trend as a function of annealing time was observed.

Keywords: skutterudite, processing, thermoelectric material.

Introduction

Filled skutterudites emerged as potential candidates for thermoelectric (TE) power generation in the 700-800 K temperature range [1]. In the case of n-type CoSb_3 , a figure of merit (ZT) exceeding unity could be achieved with suitable Yb doping [2-3]. Processing routes for obtaining the CoSb_3 single phase consist of several steps and are often time and energy consuming. Alloying of the elements can be typically obtained by ball milling (BM) [3], by continuous reaction between solid Co and liquid Sb [4] or by direct melting of the pure elements [5-6]. BM processing allows complete alloying in one step and the as milled powders are ready for subsequent compaction. However, BM processing typically favours contamination and surface oxidation of the powder. On the other hand, samples prepared from the liquid are often not homogeneous from the microstructural point of view. In fact, a complex solidification path, involving two peritectic reactions, slows down the kinetics of phases transformations. Therefore, extremely long annealing time (up to 10 days) are currently used for promoting the formation of the CoSb_3 single phase [6]. Attempts for shortening the synthesis were made by non equilibrium techniques such as rapid solidification [7-8], that also promotes nanostructuring and supersaturation of the phase with the dopant [7].

Despite the technological importance of controlling and optimizing the synthesis of CoSb_3 single phase, only few systematic studies have been carried out. For example, I.-H. Kim et al. [9] performed isochronal annealing in vacuum of undoped CoSb_3 at different temperatures between 300 °C and 800 °C. Complete formation of the single phase was achieved after annealing at 400 °C for 24 hours [9].

In this work, $\text{Yb}_{0.19}\text{Co}_4\text{Sb}_{12}$ was synthesised with a sequence of three steps: 1) a solid/liquid reaction between the pure elements; 2) complete melting in an induction furnace; 3) annealing at 730 °C. The effect of the annealing time on the evolution of phase structure and microstructure is

studied and correlated to the thermoelectric properties. It is shown that annealing for 6 hours at 730 °C promotes the formation of $\text{Yb}_{0.1}\text{Co}_4\text{Sb}_{12}$ single phase. However, the samples are characterized by a relevant amount of porosity (10-20 vol. %) that is detrimental for thermoelectric applications.

Experimental

Samples with nominal composition $\text{Yb}_{0.19}\text{Co}_4\text{Sb}_{12}$ (at.%) were prepared using elemental Co (Alfa Aesar, 99.8% powder), Sb (Alfa Aesar, 99.999% shot) e Yb (Aldrich, 99.9% chip). A small excess of Sb (about 3 at.%) was added in order to compensate the loss of this element as a consequence of its evaporation during the thermal treatments. The elements were sealed in a BN coated quartz crucible under Ar atmosphere (6.1 kPa) and were heated at 660 °C for 2.5 hours in a resistance furnace. The melting reaction was then completed in an induction furnace, under Ar atmosphere. Finally, samples in bulk form (rods with diameter 9 mm and height 30 mm) were annealed at 730 °C for 0.75, 1.5, 3 and 6 hours.

Structural analysis on ground powders obtained from the bulk samples was performed by X-ray diffraction (XRD) in transmission geometry (PANalytical X' Pert PRO, $\text{Cu K}\alpha$), using a rotating capillary. The experimental patterns were refined by Rietveld analysis using the MAUD software [10]. Microstructure and phase compositions were investigated by scanning electron microscopy (SEM) (Leica Stereoscan 420) equipped with a EDS microprobe (Oxford Instruments).

Density of the samples was measured with a picnometer.

Electrical conductivity (σ) was measured with the four-probe method. Seebeck coefficient (α) was measured with a home-made apparatus where the sample is hold between two plates. The whole sample-holder can be inserted inside a vertical electrical furnace under inert atmosphere. The temperature difference between the two plates during a heating ramp is maintained by heating the lower plate by Joule effect. Thermocouples wires were used for measuring both the temperature of the plates and the potential difference generated by the sample. The Seebeck coefficient was obtained by the following equation:

$$\alpha = \alpha_{wires} - \frac{\Delta V}{\Delta T} \quad (1)$$

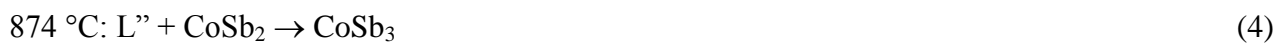
where α_{wires} represents the Seebeck coefficient of the thermocouple wires, ΔV is the measured potential difference and ΔT is the measured temperature difference. All the measurements were performed in Ar atmosphere in the temperature range between 25 °C and 300 °C.

Results and discussion

Figure 1 shows XRD patterns related to the phase evolution in the bulk samples after annealing at 730 °C for different times. The XRD pattern of the non annealed sample, clearly shows the crystallographic reflections of additional phases to CoSb_3 (Sb, CoSb and CoSb_2). As expected, increasing the annealing time, the formation of the desired CoSb_3 -type phase is promoted. The evolution of the volume fraction of the various phases is shown in Figure 2 as a function of annealing time. It can be seen that, after only 3-6 hours of annealing, the formation of the CoSb_3 -type single phase is almost completed. Table 1 shows the values of the lattice parameter for the CoSb_3 -type phase after different annealing times, together with the values of R_w indicating the quality of the fit for the Rietveld refinement. The increase of the lattice parameter with annealing time indicates that the CoSb_3 -type phase progressively solubilises a larger amount of Yb. From the comparison of the lattice parameter for the sample annealed for 6 hours ($a = 9.0462 \text{ \AA}$) with those reported in literature for undoped $\text{Co}_4\text{Sb}_{12}$ ($a = 9.0347 \text{ \AA}$ [11]) and $\text{Yb}_{0.18}\text{Co}_4\text{Sb}_{12}$ ($a = 9.0531 \text{ \AA}$ [12]), we estimated that the maximum amount of Yb solubilised in $\text{Yb}_x\text{Co}_4\text{Sb}_{12}$ is $x \sim 0.1$ indicating that the annealing is not enough for obtaining a complete dissolution (i.e. $\text{Yb}_{0.19}\text{Co}_4\text{Sb}_{12}$).

Microstructural evolution as a function of annealing time is shown by the backscattered electron SEM images in Figure 3. In the non annealed sample, Fig. 3(a), large dendrites of the primary CoSb phase are surrounded by CoSb_2 and CoSb_3 phases. CoSb, CoSb_2 and CoSb_3 are immersed in a Sb matrix. The inset of Figure 3(a) shows an eutectic microstructure consisting of YbSb_2 and Sb,

showing that Yb atoms were not fully dissolved in the skutterudite structure. After 0.75 hours of annealing, Figure 3(b), CoSb, CoSb₂ and Sb tend to disappear in favour of CoSb₃, while a small fraction of the YbSb₂/Sb eutectic is still present (see inset). After 3 hours of annealing, Figure 3(c), only residual traces of CoSb and CoSb₂ are present, whereas the YbSb₂/Sb eutectic fully disappeared. Finally, after 6 hours of annealing, the microstructure, shown in Figure 3(d), becomes more homogeneous, with only a small fraction of Sb segregated at the grain boundaries of CoSb₃. According to the Co-Sb equilibrium phase diagram [13], the sequence of reactions upon cooling is the following:



where L, L' and L'' represent the liquid phase with different compositions. The presence of significant amounts of Sb, CoSb and CoSb₂ in the non annealed sample indicates that the two peritectic reactions (3) and (4) were not completed during the non controlled cooling after induction melting, because of the long range diffusion needed. The effect of annealing is to homogenize the microstructure progressively, favouring the formation of the expected CoSb₃-type phase. The presence of residual Sb in the sample annealed for 6 hours indicates that the excess of Sb added at the beginning did not evaporated completely. All the samples show a significant amount of porosity (ranging between 10 and 20 volume %) irrespectively of the annealing time. The measured density ranges between 6.2 and 7.0 g cm⁻³, corresponding to 81-92 % of the theoretical density (7.60 g cm⁻³). According to Ref. [5], the mechanism of formation of the porosity is the following. During the peritectic reaction (3) CoSb₂ dendrites form inside the network of primary dendrites of CoSb formed from reaction (2). As a consequence of the solidification contraction, empty volumes remain between the solid phases because the pores cannot be easily filled by the remaining liquid. Since the pore fraction does not show a trend with annealing time, it can be supposed that porosity is caused by the mechanism described in Ref. [5] rather than from the evaporation of Sb. This is also

supported by the fact that the excess of Sb was not fully eliminated, as evidenced in Figure 3(d).

Finally, pores tend to become more rounded as the annealing time increases as an effect of the reduction of the surface area.

The results of thermoelectric properties are reported in Fig. 4. The evolution of the Seebeck coefficient, α , and of the electrical conductivity, σ , measured at different temperatures, as a function of the annealing time is reported in Figure 4(a) and 4(b), respectively. The Seebeck coefficient is initially positive and progressively becomes negative as the annealing proceeds. Values around $-120 \mu\text{V/K}$ and $-160 \mu\text{V/K}$ at 300 K and 500 K, respectively, are reached after annealing for 6 h. This trend is due, on the one hand, to the progressive formation of the CoSb_3 -type thermoelectric phase, and, on the other hand, to the doping of this phase with Yb, as shown by the progressive increase of the lattice parameter (table 1). In fact, undoped CoSb_3 has p-type behaviour whereas Yb-doped CoSb_3 has n-type behaviour. After annealing for 6 hours, the formation of the CoSb_3 -type phase is almost completed, whereas the Seebeck coefficient does not reach a saturation value because $\text{Yb}_x\text{Co}_4\text{Sb}_{12}$ is only partially doped with Yb, indicating that the solubilisation of Yb is a slower process with respect to the formation of the CoSb_3 -type phase.

For each annealing time, the absolute value of the Seebeck coefficient becomes larger at higher temperature, revealing the typical behaviour of doped semiconductors. The magnitude of the Seebeck coefficient obtained for the sample annealed for 6 h is slightly lower than those reported in the literature for the Yb-doped CoSb_3 single phase compound. For example, values ranging from $-130 \mu\text{V/K}$ to $-160 \mu\text{V/K}$ at 300 K, and from $-170 \mu\text{V/K}$ to $-200 \mu\text{V/K}$ at 500 K were reported in Ref. [5, 7, 14, 15]. The difference between our results and those reported in the literature is likely due to the incomplete solubilisation of Yb ($x \sim 0.1$) and to the presence of a small fraction of Sb, that shows metallic behaviour.

In the case of electrical conductivity, there is not a clear trend as a function of annealing time. The significant scattering of the values is mainly due to the high porosity of the samples, that affects the reliability of the resistivity measurements. The values obtained are slightly higher than those

typically reported for this system (e.g., between 8 and 15 10^4 S/m at 300 K [5, 7, 14, 15]). As expected, for each annealing time, the electrical conductivity decreases as the temperature increases, indicating a degenerated semiconductor behaviour due to the Yb-doping.

Comparing the results of thermoelectric properties (Figure 4) with structural and microstructural analysis of crystalline phases present in the samples as a function of annealing time (Figures 1, 2 and 3), it appears clear that, with the proposed preparation process, short annealing times (i.e. 3-6 hours) might be sufficient to obtain a single phase material. However, annealing for 6 hours at 730 °C does not allow the complete solubilisation of Yb. Furthermore, the volume contraction upon solidification leads to undesired porosity (10-20 vol. %) and, consequently, to a relative density lower than 92 % with respect to the theoretical one. Thus, improvements are needed for optimizing the preparation and annealing sequence, in order to increase the final properties.

Conclusions

In this work, $\text{Yb}_{0.19}\text{Co}_4\text{Sb}_{12}$ alloy was prepared by a combination of liquid/solid reaction, induction melting and annealing. Samples with about 98% of the desired CoSb_3 -type phase were obtained after annealing for 3-6 hours. After annealing for 6 h, the samples have an effective composition of $\text{Yb}_{0.1}\text{Co}_4\text{Sb}_{12}$ and show a chemically homogeneous microstructure, apart from a small fraction Sb in excess that segregated at the grain boundaries. All the samples show porosity ranging between 10 and 20 vol. %.

Concerning thermoelectric properties, on the one hand, the absolute value of the Seebeck coefficient progressively increases as a function of annealing time. Thermoelectric n-type behaviour reveals that the CoSb_3 -type phase was successfully doped with Yb during the annealing. On the other hand, electrical conductivity does not show a clear trend with annealing because of the porosity of the samples that leads to a density that is 81-92 % of the theoretical one. It can be concluded that the processing route proposed in this work might be effective for preparing single

phase CoSb₃-based alloys for thermoelectric applications. However, improvements are needed for ensuring a higher density of the material and a complete solubilisation of Yb.

References

- [1] C. Uher, in Semiconductors and semimetals (vol. 69), ed. by T.M. Tritt (Academic Press, 2001), pp. 139-253.
- [2] G. S. Nolas, M. Kaeser, R. T. Littleton, T. M. Tritt, Appl. Phys. Lett. 77, 1855 (2000).
- [3] J. Yang, Q. Hao, H. Wang, Y.C. Lan, Q.Y. He, A. Minnich, D.Z. Wang, J.A. Harriman, V.M. Varki, M.S. Dresselhaus, G. Chen, Z.F. Ren, Phys. Rev. B 80, 115329 (2009).
- [4] G.S. Nolas, J.L. Cohn. G.A. Slack, Phys. Rev. B 58, 164 (1998).
- [5] H.Y. Geng, S. Ochi, J.Q. Guo, Appl. Phys. Lett. 91, 022106 (2007).
- [6] Z. Xiong, X. Chen, X. Huang, S. Bai, L. Chen, Acta Mater. 58, 3995 (2010).
- [7] H. Li, X. Tang, Q. Zhang, C. Uher, Appl. Phys. Lett. 93, 252109 (2008)
- [8] Y.G. Yan, W. Wong-Ng, J.A. Kaduk, G.J. Tan, W.J. Xie, X.F. Tang, Appl. Phys. Lett. 98, 142106 (2011).
- [9] I.-H. Kim, G.-S. Choi, M.G. Han, J.-S. Kim, J.-I. Lee, S.-C. Ur, T.-W. Hong, Y.-G. Lee, S.-L. Ryu, Mater. Sci. Forum 449-452, 917 (2004).
- [10] <http://www.ing.unitn.it/~maud/>
- [11] Pearson's Handbook of Crystallographic Data for Intermetallic Phases (vol. 2), ed. by P. Villars and L.D. Calvert (American Society for Metals, Metals Park, 1985), p. 1825.
- [12] Z. Xiong, X. Chen, X. Huang, S. Bai, L. Chen, Acta Mater. 58, 3995 (2010).
- [13] H. Okamoto, Phase diagram binary alloys (American Society for Metals, Metals Park, 2000).
- [14] H. Li, X. Tang, Q. Zhang, J. Electron. Mater. 38, 1224 (2009).
- [15] H. Li, X. Tang, X. Su, Q. Zhang, C. Uher, J. Phys. D: Appl. Phys. 42, 145409 (2009).

Tables

Table 1. Values of the lattice parameter, a , of $\text{Yb}_x\text{Co}_4\text{Sb}_{12}$ and R_w for the Rietveld refinement of the X-ray diffraction patterns at different annealing times.

Annealing time (hours)	Lattice parameter of $\text{Yb}_x\text{Co}_4\text{Sb}_{12}$, a (Å)	R_w (%)
0	9.0403	2.5
0.45	9.0422	5.8
1.5	9.0428	5.4
3	9.0455	3.9
6	9.0462	6.1

Figures captions

Fig. 1. X-ray diffraction patterns for $\text{Yb}_x\text{Co}_4\text{Sb}_{12}$ for selected annealing times. Scattered curves: experimental patterns; continuous curves: fitted patterns.

Fig. 2. Evolution of the phases volume fraction as a function of annealing time.

Fig. 3. SEM backscattered electron images of the microstructure evolution in $\text{Yb}_x\text{Co}_4\text{Sb}_{12}$ at different annealing times: (a) 0 h; (b) 0.75h; (c) 3h; (d) 6h. The numbers in the micrographs indicate the corresponding phases: (1) CoSb_3 ; (2) CoSb_2 ; (3) CoSb ; (4) Sb ; (5) YbSb_2 .

Fig. 4. Thermoelectric properties of $\text{Yb}_x\text{Co}_4\text{Sb}_{12}$. Seebeck coefficient (a) and electrical conductivity (b) as a function of annealing time.

Figure 1

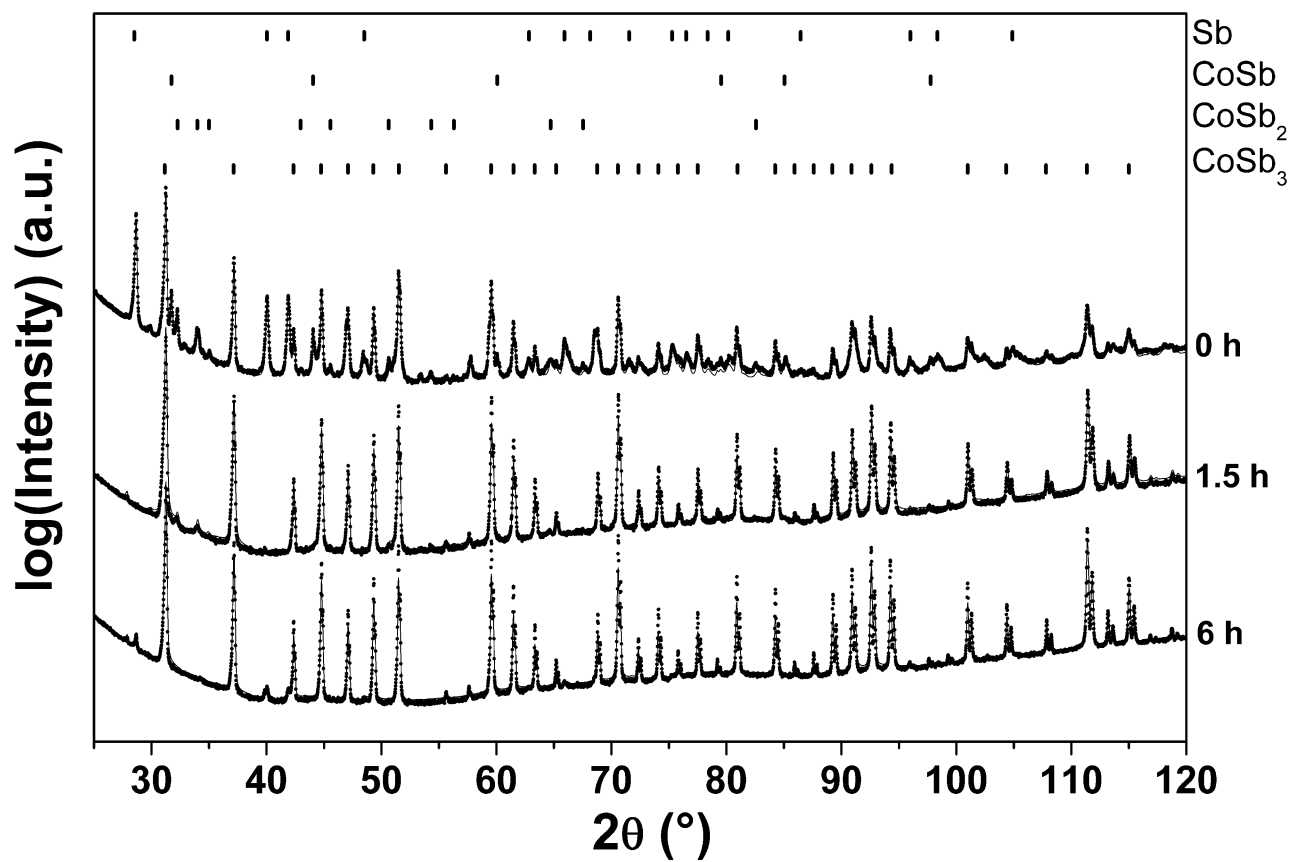


Figure 2

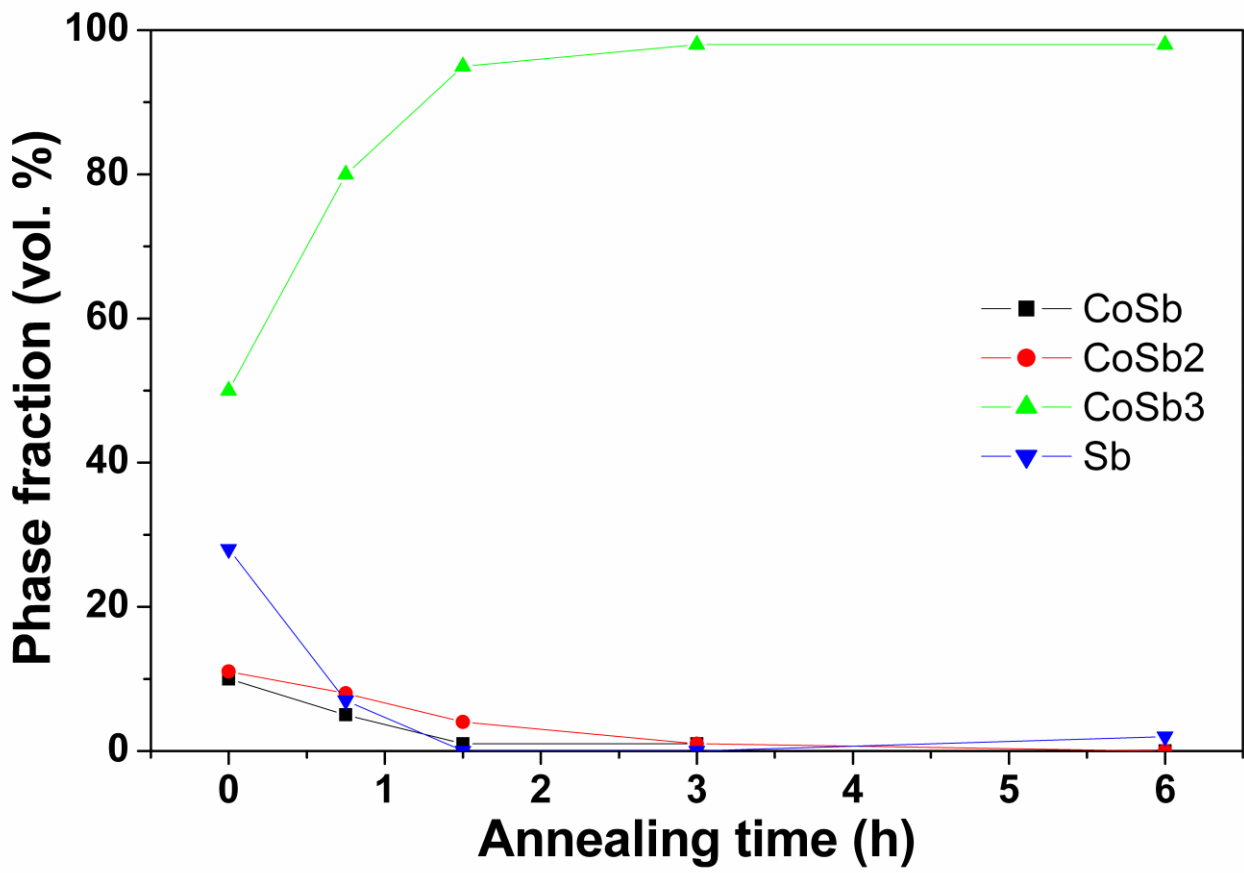


Figure 3

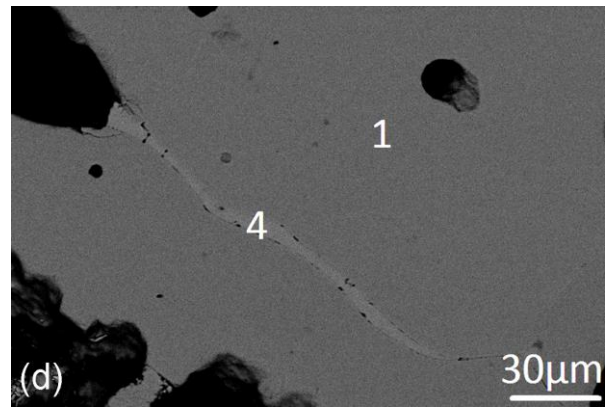
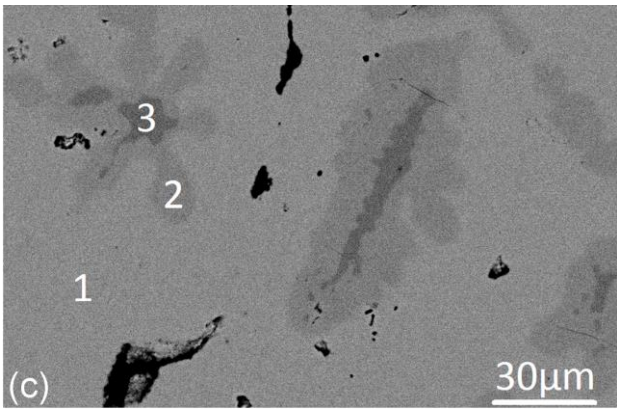
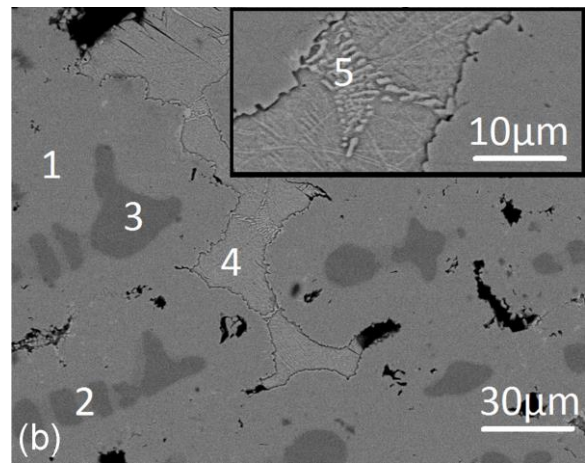
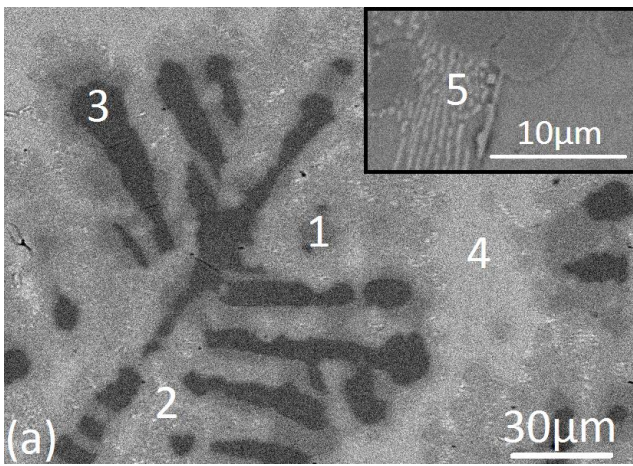


Figure 4

